Supplementary material

Enhanced CO poisoning resistance and hydrogen storage in Palladium/Metal-organic framework composites

Li Hu[a], Degao Wang[a], Feilong Yang[a], Yaqi Song[a], Manquan Fang[a], Xin Xiang[a], Renjin Xiong[a], Guikai Zhang[a], Xiaolong Wang[a]*, Tao Tang[ab]*

[a] Institute of Materials, China Academy of Engineering Physics, P. O. Box 9071-12, Mianyang 621907, China

[b] Science and Technology on Surface Physics and Chemistry Laboratory, Mianyang 621907, China

Email: tangtao@caep.cn, wangxiaolong@caep.cn

Content

Table S1 Textural properties of MOF-74(Ni) and Pd/ MOF-74(Ni).....2

Fig. S1 Survey spectrum of MOF-74(Ni) and 1 wt.%, 5 wt.% and 10 wt.% Pd/MOF-74(Ni).....2

Fig. S2 SEM morphologies of (a) MOF-74(Ni), (b-d) 1 wt.%, 5 wt.% and 10 wt.% Pd/MOF-74(Ni).....2

Fig. S3 TEM images Pd NPs (a) low magnification and (b) high magnification, (c) SAED pattern. 3

Fig. S4 The SEM image of sponge palladium 3

Table S2 Dual Site Langmuir (DSL) model fitting parameter for CO on MOF-74(Ni) 3

Fig. S5 (a) the fitting curves under different temperature; (b) $-Q_{st}$ fitting curve of CO absorption capacity at 0.5 mmol/g of MOF-74(Ni) 4

Fig. S6 The TG curve of MOF-74(Ni).....4

Fig. S7 Isothermal hydrogen absorption kinetics curve of Pd NPs at 293 K in H_2 and CO/H_2=0.1%. 4

Table S3 Saturated hydrogen absorption and the time required to reach equilibrium (t_e) of different Pd NPs loading content in different CO concentration 5

Fig. S8 The H_2 absorption curves of sponge palladium in 1% CO atmosphere at different temperatures 5

Fig. S9 The H_2 absorption curves of Pd/MOF-74(Ni) in different CO concentration (a) H_2 (b) 0.1% CO, (c) 1% CO, (d) 5% CO at 293 K 6

Fig. S10 The H_2 absorption curves of Pd/MOF-74(Ni) at different temperatures (a) 278 K, (b) 293 K, (c) 313 K, (d) 333 K in 1% CO concentration atmosphere 6

Table S4 Fitting results of JMAK model of 1 wt.% Pd/MOF-74(Ni) 7

Table S5 Fitting results of E_a of 1 wt.% Pd/MOF-74(Ni) 7

Fig. S11 Fitting curves of E_a according to JMAK model of Pd/MOF-74(Ni) with 1 wt.%, 5 wt.%, and 10 wt.% Pd NP loading.....8

Table S6 Saturated hydrogen absorption and the time required to reach equilibrium (te) of different Pd NPs at the 5th cycle in 1% CO concentration at 293 K.....8

Table S7 Textural properties of Pd/ MOF-74(Ni) after 5 recycles.....8

Fig. S12 TEM imagines of 10 wt.% Pd/MOF-74(Ni) (a) micro morphology, (b) average of Pd particle size histogram. 9

Fig. S13 *In-situ* DRIFTS spectrums of (a) Pd and (b) MOF-74(Ni) during the heating process after CO absorption9

Table S1 Textural properties of MOF-74(Ni) and Pd/ MOF-74(Ni)

Sample	S_{BET} (m^2/g)	V_{pore} (cm^3/g)	D_{pore} (Å)
MOF-74(Ni)	1121	0.49	12
1 wt.% Pd/ MOF-74(Ni)	682	0.26	15
5 wt.% Pd/ MOF-74(Ni)	247	0.18	29
10 wt.% Pd/ MOF-74(Ni)	81	0.012	35

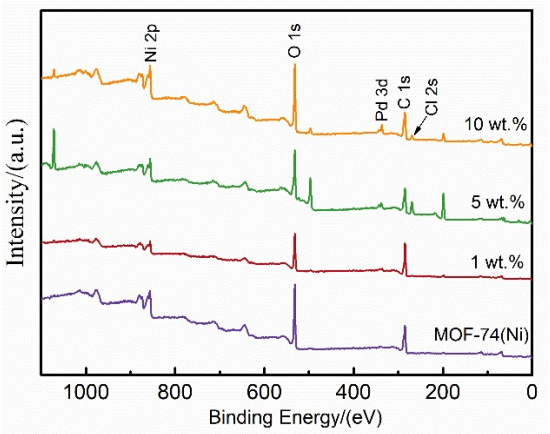

Fig. S1 Survey spectrum of MOF-74(Ni) and 1 wt.%, 5 wt.% and 10 wt.% Pd/MOF-74(Ni)

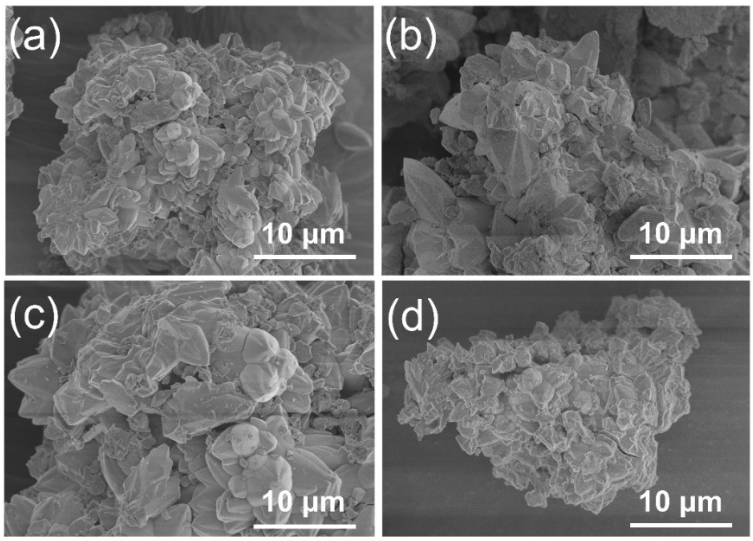

Fig. S2 SEM morphologies of (a) MOF-74(Ni), (b-d) 1 wt.%, 5 wt.% and 10 wt.% Pd/MOF-74(Ni)

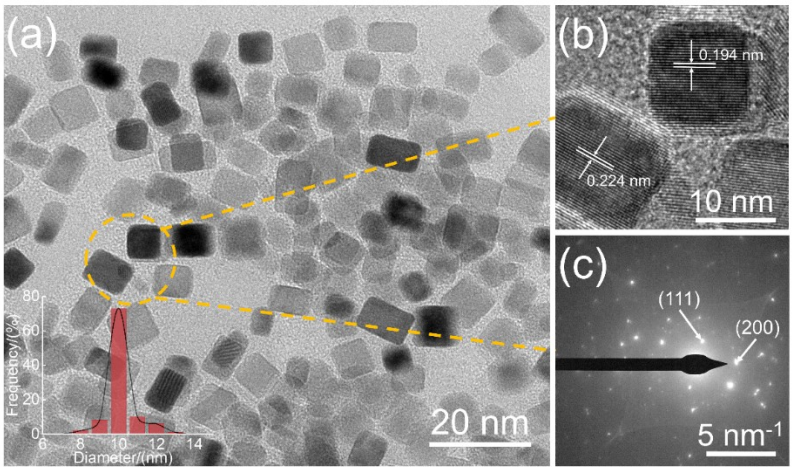

Fig. S3 TEM images Pd NPs (a) low magnification and (b) high magnification, (c) SAED pattern.

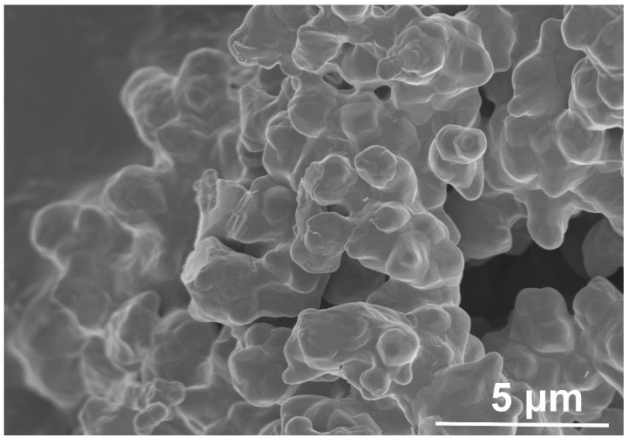

Fig. S4 The SEM image of sponge palladium

Table S2 Dual Site Langmuir (DSL) model fitting parameter for CO on MOF-74(Ni)

Temperature / K	Fitting parameter				
	q_1	k_1	q_2	k_2	R^2
278	2.12	26.24	2.72	0.38	0.997
293	2.17	18.65	2.59	0.29	0.998
303	1.84	4.64	2.85	0.22	0.998
313	3.85	0.45	0.95	0.03	0.999

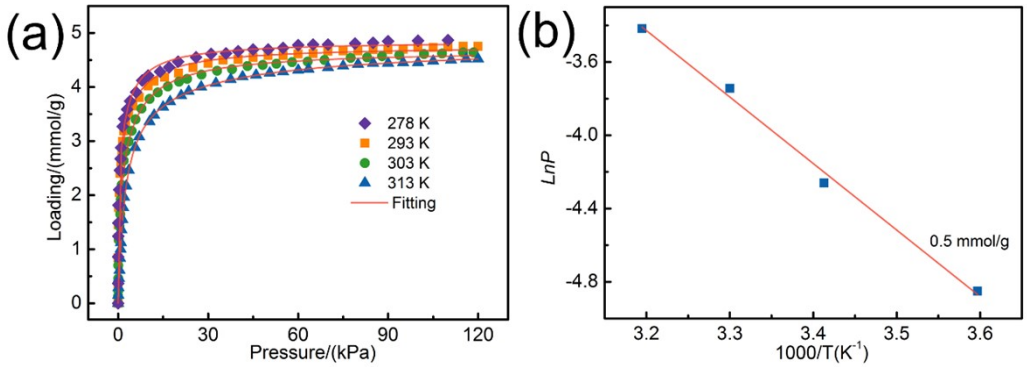

Fig. S5 (a) the fitting curves under different temperature; (b) $-Q_{st}$ fitting curve of CO absorption capacity at 0.5 mmol/g of MOF-74(Ni)

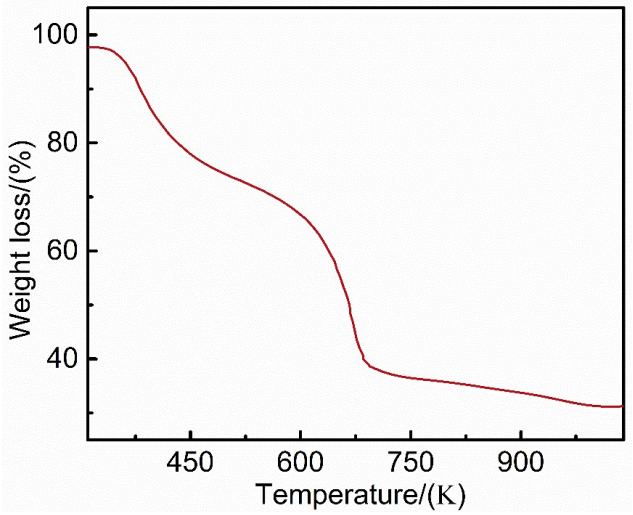

Fig. S6 The TG curve of MOF-74(Ni)

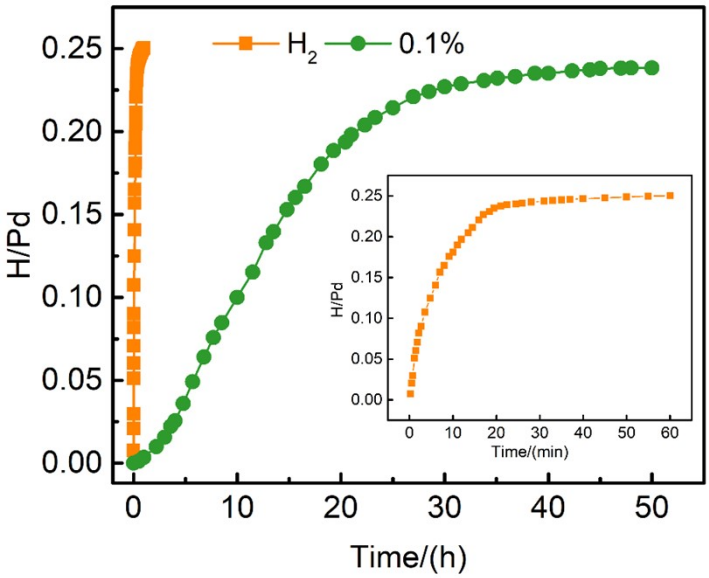

Fig. S7 Isothermal hydrogen absorption kinetics curve of Pd NPs at 293 K in H_2 and CO/H_2=0.1%.

Table S3 Saturated hydrogen absorption and the time required to reach equilibrium (t_e) of different Pd NPs loading content in different CO concentration

		H_2	0.1% CO	1% CO	5% CO
1 wt.%	max H/Pd	0.78	0.75	0.72	0.70
	t_e	150 s	1000 s	2450 s	4150 s
5 wt.%	max H/Pd	0.75	0.73	0.71	0.68
	t_e	125 s	2300 s	2800 s	5250 s
10 wt.%	max H/Pd	0.70	0.70	0.69	0.66
	t_e	75 s	2600 s	3520 s	6500 s
Pd	max H/Pd	0.65	0.65	0.64	0.56
	t_e	30 s	5.5 h	30 h	150 h

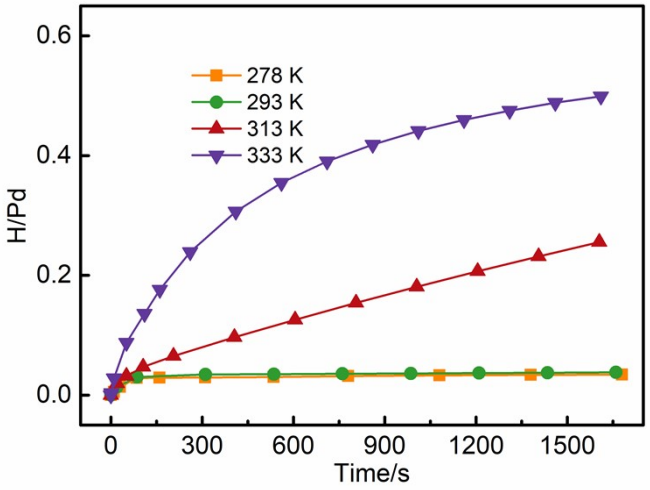

Fig. S8 The H_2 absorption curves of sponge palladium in 1% CO atmosphere at different temperatures

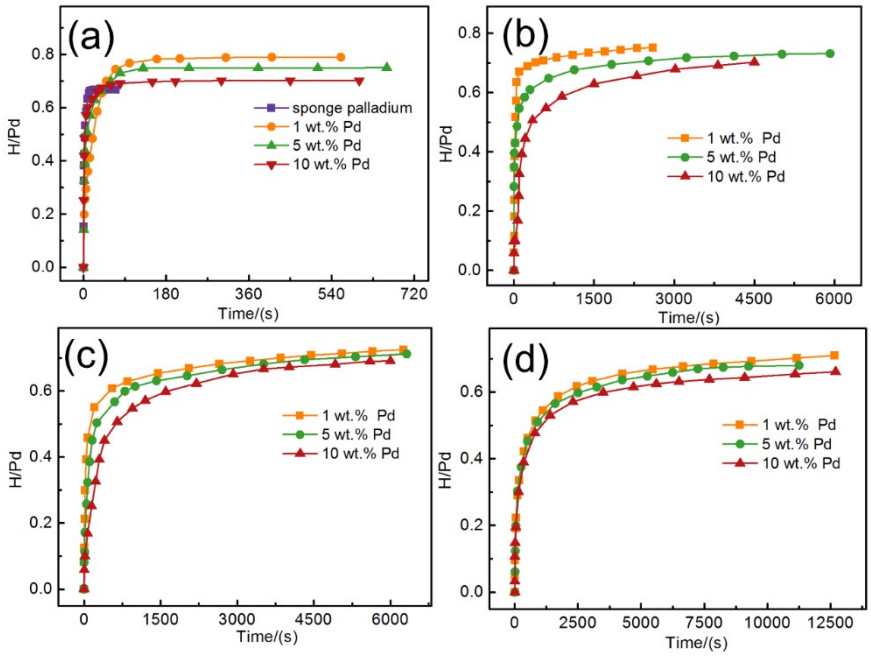

Fig. S9 The H_2 absorption curves of Pd/MOF-74(Ni) in different CO concentration (a) H_2 (b) 0.1% CO, (c) 1% CO, (d) 5% CO at 293 K

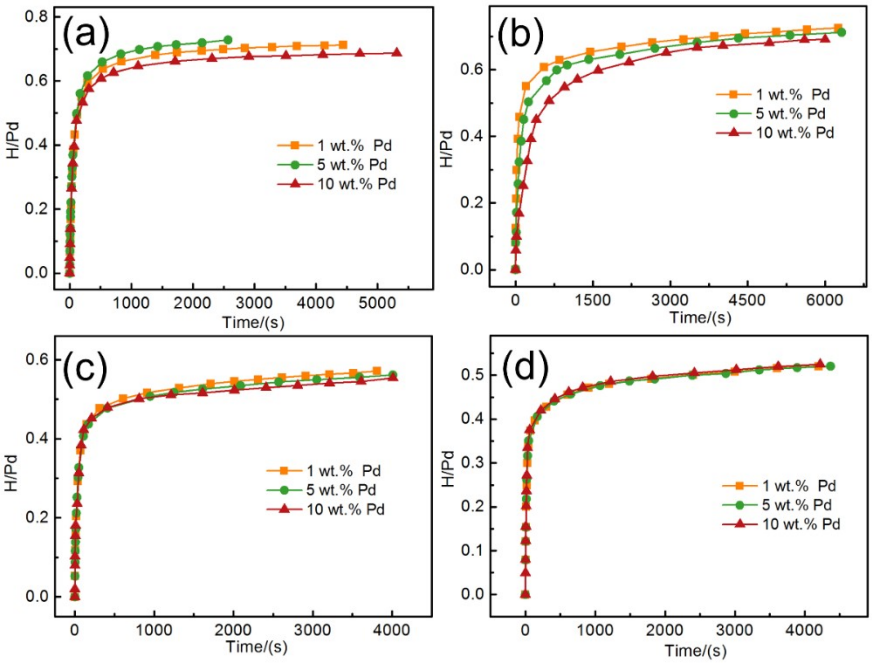

Fig. S10 The H_2 absorption curves of Pd/MOF-74(Ni) at different temperatures (a) 278 K, (b) 293 K, (c) 313 K, (d) 333 K in 1% CO concentration atmosphere

Table S4 Fitting results of JMAK model of 1 wt.% Pd/MOF-74(Ni)

Pd loading content	Temperature/(K)	Fitting equation	R^2
1 wt.%	278	y=0.57×t-2.65	0.992
	290	y=0.46×t-2.06	0.991
	313	y=0.46×t-1.93	0.989
	333	y=0.52×t-1.62	0.981
5 wt.%	278	y=0.60×t-3.11	0.997
	290	y=0.57×t-2.84	0.989
	313	y=0.50×t-2.2	0.986
	333	y=0.39×t-1.59	0.985
10 wt.%	278	y=0.78×t-4.57	0.993
	290	y=0.73×t-3.81	0.991
	313	y=0.43×t-1.95	0.980
	333	y=0.41×t-1.66	0.981

Table S5 Fitting results of E_a of 1 wt.% Pd/MOF-74(Ni)

Pd loading content	Fitting equation	R^2
1 wt.%	y= -1.02x-0.97	0.99
5 wt.%	y= -1.8x+1.54	0.99
10 wt.%	y= -3.09x+5.29	0.99

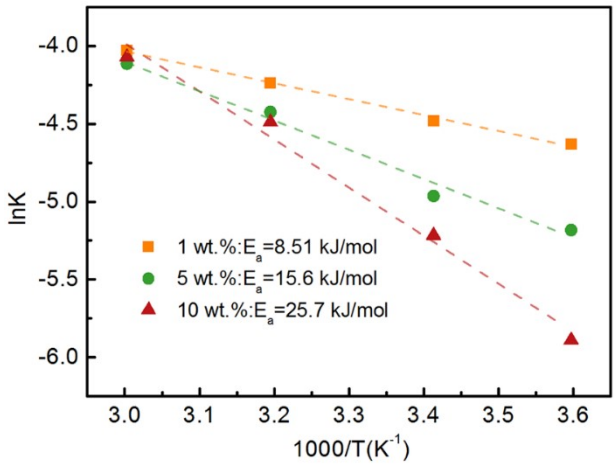

Fig. S11 Fitting curves of E_a according to JMAK model of Pd/MOF-74(Ni) with 1 wt.%, 5 wt.%, and 10 wt.% Pd NP loading

Table S6 Saturated hydrogen absorption and the time required to reach equilibrium (te) of different Pd NPs at the 5th cycle in 1% CO concentration at 293 K

Sample	max H/Pd	t_e
1 wt.% Pd/ MOF-74(Ni)	0.72	2470 s
5 wt.% Pd/ MOF-74(Ni)	0.71	2850
10 wt.% Pd/ MOF-74(Ni)	0.67	4530 s

Table S7 Textural properties of Pd/ MOF-74(Ni) after 5 recycles

Sample	S_{BET} (m^2/g)	V_{pore} (cm^3/g)	D_{pore} (Å)
1 wt.% Pd/ MOF-74(Ni)	675	0.24	16
5 wt.% Pd/ MOF-74(Ni)	239	0.17	31
10 wt.% Pd/ MOF-74(Ni)	28	0.009	64

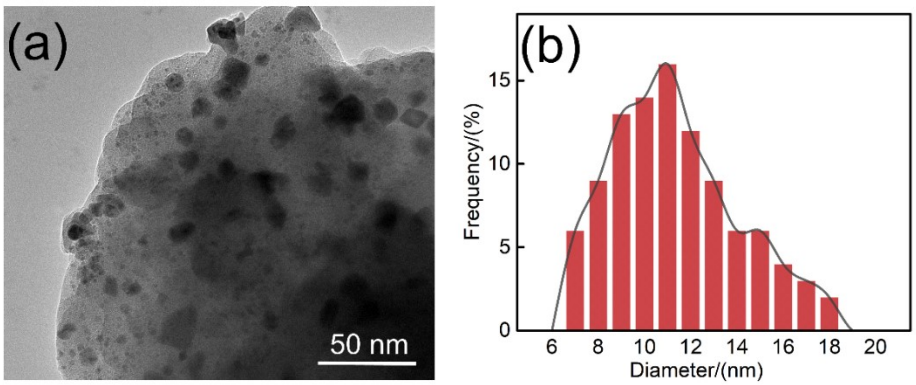

Fig. S12 TEM imagines of 10 wt.% Pd/MOF-74(Ni) (a) micro morphology, (b) average of Pd particle size histogram.

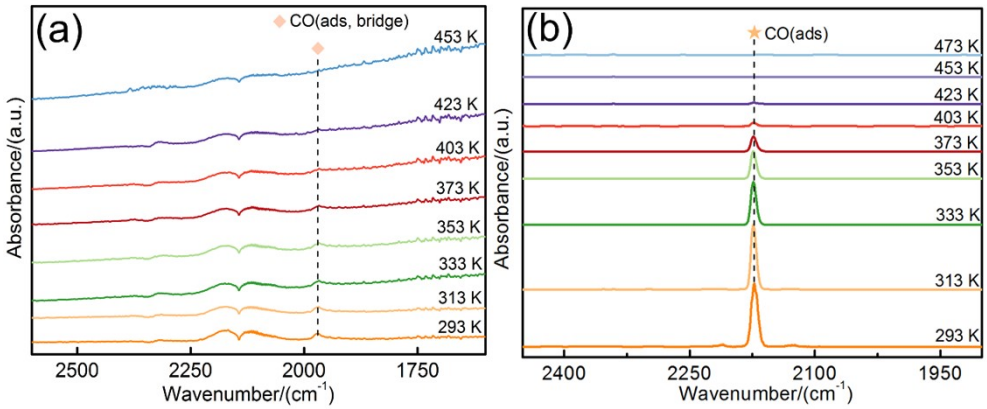

Fig. S13 *In-situ* DRIFTS spectrums of (a) Pd and (b) MOF-74(Ni) during the heating process after CO absorption